

Doubly-heavy tetraquarks

Gang Yang,^{1,*} Jialun Ping,^{2,†} and Jorge Segovia^{3,‡}

¹*Department of Physics and State Key Laboratory of Low-Dimensional Quantum Physics,
Tsinghua University, Beijing 100084, P. R. China*

²*Department of Physics and Jiangsu Key Laboratory for Numerical Simulation of Large Scale Complex Systems,
Nanjing Normal University, Nanjing 210023, P. R. China*

³*Departamento de Sistemas Físicos, Químicos y Naturales,
Universidad Pablo de Olavide, E-41013 Sevilla, Spain*

In the framework of the chiral quark model along with complex scaling range, we perform a dynamical study on the low-lying S -wave doubly-heavy tetraquark states ($QQ\bar{q}\bar{q}$, $Q = c, b$ and $q = u, d$) with an accurate computing approach, Gaussian expansion method. The meson-meson and diquark-antidiquark configurations within all possible color structures for spin-parity quantum numbers $J^P = 0^+, 1^+$ and 2^+ , and in the 0 and 1 isospin sectors are considered. Possible tightly bound and narrow resonance states are obtained for doubly-charm and doubly-bottom tetraquarks with $IJ^P = 01^+$, and these exotic states are also obtained in charm-bottom tetraquarks with 00^+ and 01^+ quantum numbers. Only loosely bound state is found in charm-bottom tetraquarks of 02^+ states. All of these bound states within meson-meson configurations are loosely bound whether in color-singlet channels or coupling to hidden-color ones. However compact structures are available in diquark-antidiquark channels except for charm-bottom tetraquarks in 02^+ states.

I. INTRODUCTION

The story of exotic hadronic states can be dated back to the announcement of $X(3872)$ in the invariant mass spectrum of $J/\psi\pi^+\pi^-$ produced in $B^\pm \rightarrow K^\pm X(3872) \rightarrow K^\pm J/\psi\pi^+\pi^-$ decays by the Belle Collaboration in 2003 [1]. This charmonium-like state was confirmed by other experimental collaborations [2–4] during the following years. However, theoretical explanations on $X(3872)$ are still controversial: (i) in spite of the predicted mass of $\chi_{c1}(2P)$ is too high (~ 3.95 GeV) to identified with $X(3872)$ [5–8], the radiative decays are better described in charmonium structure [9, 10], (ii) mass near the $D^0\bar{D}^{*0}$ threshold is compatible with molecular state [11–14] and the comprehensible isospin breaking decay process of $X(3872) \rightarrow J/\psi\rho$, (iii) the $X(3872)$ is also described as a compact diquark-antidiquark state [15], and (iv) the existence of $c\bar{c}$ bound states dressed by DD^* molecular component is proposed [16–20]. In fact, during the past 16 years, more than two dozens of unconventional charmonium- and bottomonium-like states, the so-called XYZ mesons, have been observed at B-factories (BaBar, Belle and CLEO), τ -charm facilities (CLEO-c and BESIII) and also proton-(anti)proton colliders (CDF, D0, LHCb, ATLAS and CMS), *e.g.* $Y(4260)$ discovered by the BaBar Collaboration in 2005 [21], $Z^+(4430)$ discovered by the Belle Collaboration in 2007 [22], $Y(4140)$ discovered by the CDF Collaboration in 2009 [23], and $Z_c^+(3900)$ discovered by the BESIII Collaboration in 2013 [24], *etc.* Meanwhile, remarkable achievements in the baryon

sectors are also valuable. In 2015 two exotic hidden-charmonium pentaquarks, $P_c^+(4380)$ and $P_c^+(4450)$ were announced by the LHCb Collaboration [25] in the Λ_b^0 decay, $\Lambda_b^0 \rightarrow J/\psi K^- p$ and in 2019 with higher statistical significance, one new pentaquark state $P_c^+(4312)$ was found by the same collaboration and the previously reported wide state $P_c^+(4450)$ was superseded by two narrow ones, $P_c^+(4440)$ and $P_c^+(4457)$ [26]. Review on these exotic states can be found in Ref. [27–30].

Apparently, these facts have triggered large amount of theoretical investigations on the new hadronic zoo where the conventional configuration of mesons and baryons as, respectively, quark-antiquark and 3-quark bound states is being left behind. In fully-heavy tetraquarks sector, the CMS collaboration claimed an observation of pair production of $\Upsilon(1S)$ mesons at the LHC in pp collisions [31] and this may indicated a $b\bar{b}b\bar{b}$ tetraquark state with mass of 18.4 GeV. A significant peak at ~ 18.2 GeV was observed in Cu+Au collisions at RHIC [32]. However, no evidence has been provided from the LHCb collaboration by searching for the $\Upsilon(1S)\mu^+\mu^-$ invariant mass spectrum [33]. Extensive theoretical works with different schemes devote to these extremely non-relativistic systems, $QQ\bar{Q}\bar{Q}$ ($Q = c, b$): the existence of $b\bar{b}b\bar{b}$ bound state is supported by phenomenological model calculation [34–37], QCD sum rules [38, 39], and diffusion Monte Carlo method [40]. A narrow $cc\bar{c}\bar{c}$ tetraquark state in the mass region 5 – 6 GeV has been predicted by the Bethe-Salpeter approach [41] and also in several phenomenological models [34, 42–44]. However, there are still intense debates on the observation of these exotic states. No $cc\bar{c}\bar{c}$ and $b\bar{b}b\bar{b}$ bound states can be formed within effective model calculations [45–50] and lattice QCD [51], but possible stable or narrow states in the $b\bar{b}b\bar{c}$ and $bcb\bar{c}$ systems [45, 46].

Nevertheless, results on doubly-heavy tetraquark states investigated by different kinds of theoretical ap-

* ygz0788a@sina.com

† jlping@njnu.edu.cn

‡ jsegovia@upo.es

proaches are more compatible. In heavy quark limit, stable and extremely narrow $bb\bar{u}\bar{d}$ tetraquark state with the $J^P = 1^+$ must exist [52]. In Ref. [53] the predicted mass of $bb\bar{u}\bar{d}$ state within the same spin-parity is 10389 ± 12 MeV. Mass, lifetime and decay modes of this tetraquark are investigated in Ref. [54]. A compact doubly-bottom tetraquark state with $IJ^P = 01^+$ is also presented in heavy-ion collisions at the LHC [55] and actually, in 1988 the dimeson $T(bb\bar{u}\bar{d})$ had already been proposed [56]. Besides, a narrow $(bb)(\bar{u}\bar{d})$ diquark-antidiquark state with $IJ^P = 01^+$ is predicted in Ref. [57]. A $bbud$ bound state also with $IJ^P = 01^+$ is stable against the strong and electromagnetic decay and its mass is $10476 \pm 24 \pm 10$ MeV by Lattice QCD [58], this deeply bound state is supported also by the same formalism in Refs. [59, 60]. Meanwhile, there are also QCD sum rules predicted a mass 7105 ± 155 MeV for $bc\bar{u}\bar{d}$ axial-vector tetraquark state [61], and $I(J^P) = 0(1^+) u\bar{d}\bar{c}\bar{d}$ tetraquark which binding energy is 15 to 61 MeV with respect to $\bar{D}B^*$ threshold is proposed by Ref. [62]. Moreover, the production potential of doubly-heavy tetraquarks at a Tera-Z factory and the LHC are estimated by Monte Carlo simulation [63, 64]. However, no strong indication for any bound state or narrow resonance of tetraquarks in charm sector are found in Lattice study [65]. Some other types of tetraquark states along with decay properties are explored in Refs. [66–68].

We study herein, within a complex scaling range of chiral quark model formalism, the possibility of having tetraquark bound- and resonance-states in the doubly-heavy sector with quantum numbers $J^P = 0^+, 1^+$ and 2^+ , and in the 0 and 1 isospin sectors. Two configurations, meson-meson and diquark-antidiquark structures are considered. In particular, color-singlet and hidden-color channels for dimeson configuration, color triplet-antitriple and sextet-antisextet channels for diquark-antidiquark one along with their couplings are all employed for each quantum states. The bound states, if possible, their internal structures and components in the complete coupled-channels calculation are analyzed by computing the distances among any pair of quarks and the contributions of each channel's wave functions. Meanwhile, masses and widths for possible resonance states are also studied in the complete coupled-channels.

The four-body bound state problem is implemented by two strong foundations, the Gaussian expansion method (GEM) [69] which has been demonstrated to be as accurate as a Faddeev calculation (see, for instance, Figs. 15 and 16 of Ref. [69]), and the chiral quark model which has been successfully applied to hadron [8, 70–75], hadron-hadron [76–80] and multiquark [81–84] phenomenology. However, due to the complexity of the coupled channels case for scattering and resonance states, it is difficult to solve a scattering issue together with resonance one. In this work, a powerful technique, complex scaling method (CSM) is employed, and this is also for the first time that its application to tetraquark states in hadronic physics. During the past decades, it has been extensively applied

to nuclear physics problems [85, 86], and recently also in the study of charmed dibaryon resonances [87]. The CSM is quite different from a real range one, for the scattering, resonance and bound states can all be concordant in one calculation (see Fig. 1, a schematic distribution of the complex energy of 2-body by the CSM according to Ref. [86]), namely the scattering states can be solved as a bound states problem without Lippmann-Schwinger equation or some scattering issues related, and the resonance pole will be fixed in the complex plane. A briefly sketch for the application of CSM in tetraquark states will be shown in the next section.

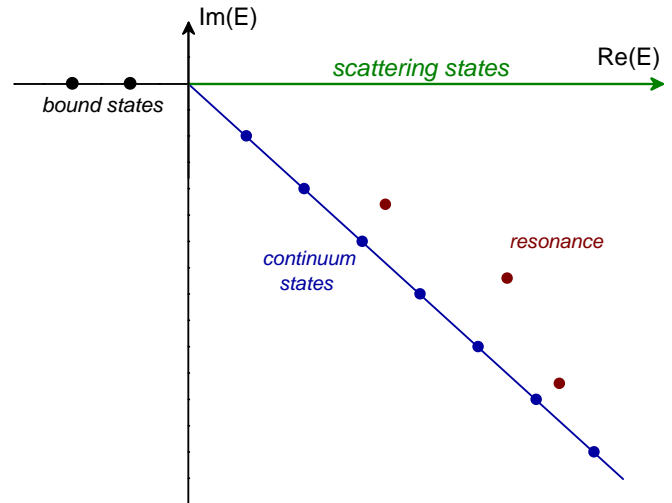


FIG. 1. Schematic complex energy distribution in the single-channel two-body system.

The structure of this paper is organized in the following way. In Sec. II theoretical framework which includes the ChQM, tetraquark wave-functions, GEM and CSM is briefly presented and discussed. Section III is devoted to the analysis and discussion on the obtained results. The summary and some prospects are presented in Sec. IV.

II. THEORETICAL FRAMEWORK

With half a century development in high energy physics, the QCD-inspired quark models are still the main tool to shed some light on the nature of the multiquark candidates observed by experimentalists. Particularly, the chiral quark model has been witnessed great achievements in our early work on possible hidden-charm pentaquark bound states with quantum numbers $IJ^P = \frac{1}{2}(\frac{1}{2})^\pm, \frac{1}{2}(\frac{3}{2})^\pm$ and $\frac{1}{2}(\frac{5}{2})^\pm$ [82]. Therein, the properties were compared with those associated with the hidden-charm pentaquark signals observed by the LHCb Collaboration in 2015 [25]. Although three new hidden-charm pentaquarks were also reported by the same collaboration in 2019 [26], these states are not discussing exactly in the present work. Herein, the application of

chiral quark model in doubly-heavy tetraquark states is quite expected.

The general form of our four-body Hamiltonian in complex scaling method is

$$H(\theta) = \sum_{i=1}^4 \left(m_i + \frac{\vec{p}_i^2}{2m_i} \right) - T_{\text{CM}} + \sum_{j>i=1}^4 V(\vec{r}_{ij}e^{i\theta}), \quad (1)$$

where the center-of-mass kinetic energy T_{CM} is subtracted without losing a generality since we mainly focus on the internal relative motions of multi-quark system. Interaction part is of two-body potential

$$V(\vec{r}_{ij}e^{i\theta}) = V_{\text{CON}}(\vec{r}_{ij}e^{i\theta}) + V_{\text{OGE}}(\vec{r}_{ij}e^{i\theta}) + V_{\chi}(\vec{r}_{ij}e^{i\theta}), \quad (2)$$

includes the color-confining, one-gluon exchange and Goldstone-boson exchange interactions. Note herein that only the central and spin-spin of potential are considered since our main goal of the present work is to perform a systematical study on the low-lying S -wave doubly-heavy tetraquark states, it is reasonable for the absence of spin-orbit and tensor contributions. One can see that the coordinates of relative motions between quarks are transformed with a complex rotation, $\vec{r} \rightarrow \vec{r}e^{i\theta}$. Accordingly, in the framework of complex range, the four-body systems are solved in a complex scaled Schrödinger equation:

$$[H(\theta) - E(\theta)] \Psi_{JM}(\theta) = 0 \quad (3)$$

According to the ABC theorem [88, 89], there are three types of complex eigenenergies of Eq. (3) as shown in Fig. 1:

(1) The bound state below the threshold is always located on the negative axis of real energy.

(2) The discretized continuum state are aligned along the cut line with a rotated angle of 2θ related to the real axis.

(3) The resonance state is a fixed pole under the complex scaling transformation and is located above the continuum cut line. The resonance width is given by $\Gamma = -2\text{Im}(E)$.

As an illustration to each interaction potentials in Eq. (2). Firstly, color confinement should be encoded in the non-Abelian character of QCD. It has been demonstrated by LQCD that multi-gluon exchanges produce an attractive linearly rising potential proportional to the distance between infinite-heavy quarks [90]. However, the spontaneous creation of light-quark pairs from the QCD vacuum may give rise at the same scale to a breakup of the created color flux-tube [90]. These two phenomenological observations are mimicked by the following expression when $\theta = 0^\circ$:

$$V_{\text{CON}}(\vec{r}_{ij}e^{i\theta}) = \left[-a_c(1 - e^{-\mu_c r_{ij}e^{i\theta}}) + \Delta \right] (\vec{\lambda}_i^c \cdot \vec{\lambda}_j^c), \quad (4)$$

where a_c , μ_c and Δ are model parameters, and the SU(3) color Gell-Mann matrices are denoted as λ^c . One can

see in Eq. (4) that the potential is linear at short interquark distances with an effective confinement strength $\sigma = -a_c \mu_c (\vec{\lambda}_i^c \cdot \vec{\lambda}_j^c)$, while V_{CON} becomes constant $(\Delta - a_c)(\vec{\lambda}_i^c \cdot \vec{\lambda}_j^c)$ at large distances.

The one-gluon exchange potential which includes the coulomb and color-magnetism interactions is given by

$$V_{\text{OGE}}(\vec{r}_{ij}e^{i\theta}) = \frac{1}{4}\alpha_s(\vec{\lambda}_i^c \cdot \vec{\lambda}_j^c) \left[\frac{1}{r_{ij}e^{i\theta}} - \frac{1}{6m_i m_j} (\vec{\sigma}_i \cdot \vec{\sigma}_j) \frac{e^{-r_{ij}e^{i\theta}/r_0(\mu)}}{r_{ij}e^{i\theta} r_0^2(\mu)} \right], \quad (5)$$

where m_i and $\vec{\sigma}$ are the quark mass and the Pauli matrices respectively. The contact term of the central potential in complex range has been regularized as

$$\delta(\vec{r}_{ij}e^{i\theta}) \sim \frac{1}{4\pi r_0^2} \frac{e^{-r_{ij}e^{i\theta}/r_0}}{r_{ij}e^{i\theta}}, \quad (6)$$

with $r_0(\mu_{ij}) = \hat{r}_0/\mu_{ij}$ a regulator that depends on μ_{ij} , the reduced mass of the quark-(anti-)quark pair.

The QCD strong coupling constant α_s (an effective scale-dependent strong coupling constant) offers a consistent description of mesons and baryons from light to heavy quark sectors in wide energy range, and we use the frozen coupling constant of, for instance, Ref. [7]

$$\alpha_s(\mu_{ij}) = \frac{\alpha_0}{\ln \left(\frac{\mu_{ij}^2 + \mu_0^2}{\Lambda_0^2} \right)}, \quad (7)$$

in which α_0 , μ_0 and Λ_0 are parameters of the model.

The central terms of Goldstone-boson exchange interaction in CSM can be written as

$$V_{\pi}(\vec{r}_{ij}e^{i\theta}) = \frac{g_{ch}^2}{4\pi} \frac{m_{\pi}^2}{12m_i m_j} \frac{\Lambda_{\pi}^2}{\Lambda_{\pi}^2 - m_{\pi}^2} m_{\pi} \left[Y(m_{\pi} r_{ij}e^{i\theta}) - \frac{\Lambda_{\pi}^3}{m_{\pi}^3} Y(\Lambda_{\pi} r_{ij}e^{i\theta}) \right] (\vec{\sigma}_i \cdot \vec{\sigma}_j) \sum_{a=1}^3 (\lambda_i^a \cdot \lambda_j^a), \quad (8)$$

$$V_{\sigma}(\vec{r}_{ij}e^{i\theta}) = -\frac{g_{ch}^2}{4\pi} \frac{\Lambda_{\sigma}^2}{\Lambda_{\sigma}^2 - m_{\sigma}^2} m_{\sigma} \left[Y(m_{\sigma} r_{ij}e^{i\theta}) - \frac{\Lambda_{\sigma}}{m_{\sigma}} Y(\Lambda_{\sigma} r_{ij}e^{i\theta}) \right], \quad (9)$$

$$V_K(\vec{r}_{ij}e^{i\theta}) = \frac{g_{ch}^2}{4\pi} \frac{m_K^2}{12m_i m_j} \frac{\Lambda_K^2}{\Lambda_K^2 - m_K^2} m_K \left[Y(m_K r_{ij}e^{i\theta}) - \frac{\Lambda_K^3}{m_K^3} Y(\Lambda_K r_{ij}e^{i\theta}) \right] (\vec{\sigma}_i \cdot \vec{\sigma}_j) \sum_{a=4}^7 (\lambda_i^a \cdot \lambda_j^a), \quad (10)$$

$$V_{\eta}(\vec{r}_{ij}e^{i\theta}) = \frac{g_{ch}^2}{4\pi} \frac{m_{\eta}^2}{12m_i m_j} \frac{\Lambda_{\eta}^2}{\Lambda_{\eta}^2 - m_{\eta}^2} m_{\eta} \left[Y(m_{\eta} r_{ij}e^{i\theta}) - \frac{\Lambda_{\eta}^3}{m_{\eta}^3} Y(\Lambda_{\eta} r_{ij}e^{i\theta}) \right] (\vec{\sigma}_i \cdot \vec{\sigma}_j) \left[\cos \theta_p (\lambda_i^8 \cdot \lambda_j^8) - \sin \theta_p \right], \quad (11)$$

TABLE I. Model parameters.

Quark masses	$m_u = m_d$ (MeV)	313
	m_c (MeV)	1752
	m_b (MeV)	5100
Goldstone bosons	$\Lambda_\pi = \Lambda_\sigma$ (fm $^{-1}$)	4.20
	Λ_η (fm $^{-1}$)	5.20
	$g_{ch}^2/(4\pi)$	0.54
	$\theta_P(^{\circ})$	-15
Confinement	a_c (MeV)	430
	μ_c (fm $^{-1}$)	0.70
	Δ (MeV)	181.10
OGE	α_0	2.118
	Λ_0 (fm $^{-1}$)	0.113
	μ_0 (MeV)	36.976
	\hat{r}_0 (MeV fm)	28.170

where $Y(x) = e^{-x}/x$ is the standard Yukawa function. The physical η meson are considered by introducing the angle θ_p instead of the octet one. The λ^a are the SU(3) flavor Gell-Mann matrices. Taken from their experimental values, m_π , m_K and m_η are the masses of the SU(3) Goldstone bosons. The value of m_σ is determined through the PCAC relation $m_\sigma^2 \simeq m_\pi^2 + 4m_{u,d}^2$ [91]. Finally, the chiral coupling constant, g_{ch} , is determined from the πNN coupling constant through

$$\frac{g_{ch}^2}{4\pi} = \frac{9}{25} \frac{g_{\pi NN}^2}{4\pi} \frac{m_{u,d}^2}{m_N^2}, \quad (12)$$

which assumes that flavor SU(3) is an exact symmetry only broken by the different mass of the strange quark.

One need to mention that the chiral quark-(anti)quark interaction only play a role between two light quarks, and it is invalid for the other heavy-light and heavy-heavy quark pairs due to the isospin symmetry breaking. The model parameters which are listed in Table I have been fixed in advance reproducing hadron [8, 70–74], hadron-hadron [76–80] and multi-quark [81–84] phenomenology.

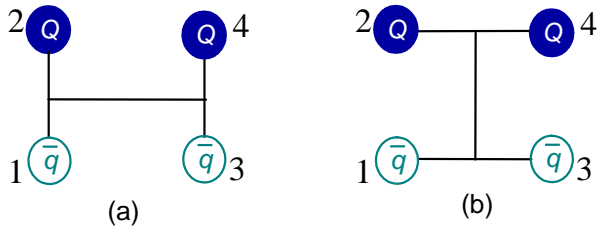


FIG. 2. Two types of configurations in doubly-heavy tetraquarks. Panel (a) is meson-meson structure and panel (b) is diquark-antidiquark one. ($Q = c, b$ and $q = u, d$)

Four fundamental degrees of freedom in quark level: color, flavor, spin and space are generally accepted

in the QCD theory and the multi-quark system wave function is a product of these four terms. In Fig. 2, we show two kinds of configurations for doubly-heavy tetraquarks $QQ\bar{q}\bar{q}$ ($q = u, d$ and $Q = c, b$). In particular, Fig. 2(a) is the meson-meson (MM) structure and diquark-antidiquark (DA) one is of Fig. 2(b), both of them and their coupling are considered in our investigation.

Concerning the color degree-of-freedom, more richer structures in multi-quark system will be discussed than conventional hadrons ($q\bar{q}$ mesons and qqq baryons). The colorless wave function of 4-quark systems in dimeson configuration can be obtained by either a color-singlet or a hidden-color channel or both. However, this is not an unique path for the authors of Refs. [92, 93] assert that it is enough to consider the color singlet channel when all possible excited states of a system are included. After a comparison, a more economical way of computing through considering all the possible color structures and their coupling is employed. Firstly, in the color SU(3) group, the wave functions of color-singlet (two color-singlet clusters coupling, 1×1) and hidden-color (two color-octet clusters coupling, 8×8) channel in dimeson configuration of Fig. 2(a) is signed as χ_1^c and χ_2^c respectively,

$$\chi_1^c = \frac{1}{3}(\bar{r}r + \bar{g}g + \bar{b}b) \times (\bar{r}r + \bar{g}g + \bar{b}b), \quad (13)$$

$$\begin{aligned} \chi_2^c = & \frac{\sqrt{2}}{12}(3\bar{b}r\bar{r}b + 3\bar{g}r\bar{r}g + 3\bar{b}g\bar{g}b + 3\bar{g}b\bar{b}g + 3\bar{r}g\bar{g}r \\ & + 3\bar{r}b\bar{b}r + 2\bar{r}r\bar{r}r + 2\bar{g}g\bar{g}g + 2\bar{b}b\bar{b}b - \bar{r}r\bar{g}g \\ & - \bar{g}g\bar{r}r - \bar{b}b\bar{g}g - \bar{b}b\bar{r}r - \bar{g}g\bar{b}b - \bar{r}r\bar{b}b). \end{aligned} \quad (14)$$

In additional, also according to an increased sequence of numbers labeled in Fig. 2, the color wave functions of diquark-antidiquark structure shown in Fig. 2(b) are χ_3^c (color triplet-antitriplet clusters coupling, $3 \times \bar{3}$) and χ_4^c (color sextet-antisextet clusters coupling, $6 \times \bar{6}$), respectively:

$$\begin{aligned} \chi_3^c = & \frac{\sqrt{3}}{6}(\bar{r}r\bar{g}g - \bar{g}r\bar{r}g + \bar{g}g\bar{r}r - \bar{r}g\bar{g}r + \bar{r}r\bar{b}b \\ & - \bar{b}r\bar{r}b + \bar{b}b\bar{r}r - \bar{r}b\bar{b}r + \bar{g}g\bar{b}b - \bar{b}g\bar{g}b \\ & + \bar{b}b\bar{g}g - \bar{g}b\bar{b}g), \end{aligned} \quad (15)$$

$$\begin{aligned} \chi_4^c = & \frac{\sqrt{6}}{12}(2\bar{r}r\bar{r}r + 2\bar{g}g\bar{g}g + 2\bar{b}b\bar{b}b + \bar{r}r\bar{g}g + \bar{g}r\bar{r}g \\ & + \bar{g}g\bar{r}r + \bar{r}g\bar{g}r + \bar{r}r\bar{b}b + \bar{b}r\bar{r}b + \bar{b}b\bar{r}r \\ & + \bar{r}b\bar{b}r + \bar{g}g\bar{b}b + \bar{b}g\bar{g}b + \bar{b}b\bar{g}g + \bar{g}b\bar{b}g). \end{aligned} \quad (16)$$

As for the flavor degree-of freedom, due to the quark contents of the present investigated 4-quark systems are two heavy quarks ($Q = c, d$) and two light antiquarks ($\bar{q} = \bar{u}, \bar{d}$), only isospin $I = 0$ and 1 will be obtained.

Moreover, the flavor wave-functions signed as $\chi_{I,M_I}^{f_i}$ with the superscript $i = 1, 2$ and 3 are of $cc\bar{q}\bar{q}$, $bb\bar{q}\bar{q}$ and $cb\bar{q}\bar{q}$ systems, respectively. The specific wave functions read as below,

$$\chi_{0,0}^{f_1} = \sqrt{\frac{1}{2}}(\bar{u}c\bar{d}c - \bar{d}c\bar{u}c), \quad (17)$$

$$\chi_{1,-1}^{f_1} = \bar{u}c\bar{u}c, \quad (18)$$

$$\chi_{0,0}^{f_2} = \sqrt{\frac{1}{2}}(\bar{u}b\bar{d}b - \bar{d}b\bar{u}b), \quad (19)$$

$$\chi_{1,-1}^{f_2} = \bar{u}b\bar{u}b, \quad (20)$$

$$\chi_{0,0}^{f_3} = \sqrt{\frac{1}{2}}(\bar{u}c\bar{d}b - \bar{d}c\bar{u}b), \quad (21)$$

$$\chi_{1,-1}^{f_3} = \bar{u}c\bar{u}b, \quad (22)$$

where the third component of the isospin M_I is set to be equal to the absolute value of total one I without loss of generality for there is no interplay in the Hamiltonian that can distinguish such component.

We consider herein 4-quark bound states with total spin S ranging from 0 to 2. Since there is not any spin-orbital coupling dependent potential included in our Hamiltonian, the third component (M_S) of tetraquark spin can be assumed to be equal to the total one without loss of generality too. Our total spin wave functions χ_{S,M_S}^σ are given by:

$$\chi_{0,0}^{\sigma_1}(4) = \chi_{00}^\sigma \chi_{00}^\sigma \quad (23)$$

$$\chi_{0,0}^{\sigma_2}(4) = \frac{1}{\sqrt{3}}(\chi_{11}^\sigma \chi_{1,-1}^\sigma - \chi_{10}^\sigma \chi_{10}^\sigma + \chi_{1,-1}^\sigma \chi_{11}^\sigma) \quad (24)$$

$$\chi_{1,1}^{\sigma_1}(4) = \chi_{00}^\sigma \chi_{11}^\sigma \quad (25)$$

$$\chi_{1,1}^{\sigma_2}(4) = \chi_{11}^\sigma \chi_{00}^\sigma \quad (26)$$

$$\chi_{1,1}^{\sigma_3}(4) = \frac{1}{\sqrt{2}}(\chi_{11}^\sigma \chi_{10}^\sigma - \chi_{10}^\sigma \chi_{11}^\sigma) \quad (27)$$

$$\chi_{2,2}^{\sigma_1}(4) = \chi_{11}^\sigma \chi_{11}^\sigma \quad (28)$$

these expressions are obtained by considering the coupling of two sub-clusters spin wave functions with SU(2) algebra, and the necessary bases are read as

$$\chi_{11}^\sigma = \alpha\alpha, \chi_{1,-1}^\sigma = \beta\beta \quad (29)$$

$$\chi_{10}^\sigma = \frac{1}{\sqrt{2}}(\alpha\beta + \beta\alpha) \quad (30)$$

$$\chi_{00}^\sigma = \frac{1}{\sqrt{2}}(\alpha\beta - \beta\alpha) \quad (31)$$

Here, one important thing need to be mentioned that the spin wave functions of Eq. (25) and (26) are equivalent for two D - or B -mesons configuration of tetraquark state. Namely, the calculated masses of DD^* and D^*D are exactly the same (also for BB^*) and obviously, this is a trivial fact in hadron level.

Among the different methods to solve the Schrödinger-like 4-body bound state equation, we use the Rayleigh-

Ritz variational principle which is one of the most extended tools to solve eigenvalue problems due to its simplicity and flexibility. Meanwhile, the choice of basis to expand the intrinsic wave function of state is of great importance. In the relative motion coordinates of 4-quark systems, the spatial wave function is written as follows:

$$\psi_{LM_L}(\theta) = \left[\left[\phi_{n_1 l_1}(\vec{\rho} e^{i\theta}) \phi_{n_2 l_2}(\vec{\lambda} e^{i\theta}) \right]_l \phi_{n_3 l_3}(\vec{R} e^{i\theta}) \right]_{LM_L}, \quad (32)$$

where the internal Jacobi coordinates for Fig. 2(a) of meson-meson configuration are defined as

$$\vec{\rho} = \vec{x}_1 - \vec{x}_2, \quad (33)$$

$$\vec{\lambda} = \vec{x}_3 - \vec{x}_4, \quad (34)$$

$$\vec{R} = \frac{m_1 \vec{x}_1 + m_2 \vec{x}_2}{m_1 + m_2} - \frac{m_3 \vec{x}_3 + m_4 \vec{x}_4}{m_3 + m_4}, \quad (35)$$

and the diquark-antidiquark structure of Fig. 2(b) are,

$$\vec{\rho} = \vec{x}_1 - \vec{x}_3, \quad (36)$$

$$\vec{\lambda} = \vec{x}_2 - \vec{x}_4, \quad (37)$$

$$\vec{R} = \frac{m_1 \vec{x}_1 + m_3 \vec{x}_3}{m_1 + m_3} - \frac{m_2 \vec{x}_2 + m_4 \vec{x}_4}{m_2 + m_4}. \quad (38)$$

Obviously, with these sets of coordinates the center-of-mass kinetic term T_{CM} can be completely eliminated for a nonrelativistic system. Besides, the Jacobi coordinates of Eq. (32) are also transformed with a common scaling angle θ .

A high efficiency and exact method in solving bound state of few-body system, Gaussian expansion method (GEM) [69] is employed in this work, all of the relative motions of 4-quark systems are expanded with various Gaussian basis which are taken as the geometric progression sizes¹, and the form of orbital wave functions, ϕ 's in Eq. (32) is

$$\phi_{nlm}(\vec{r} e^{i\theta}) = N_{nl} (r e^{i\theta})^l e^{-\nu_n (r e^{i\theta})^2} Y_{lm}(\hat{r}). \quad (39)$$

Moreover, our present study is only in S -wave state of doubly-heavy tetraquarks, no laborious Racah algebra during matrix elements calculation for the value of spherical harmonic function is a constant when $l = 0$, *i.e.* $Y_{00} = \sqrt{1/4\pi}$.

Finally, in order to fulfill the Pauli principle, the complete wave-function is written as

$$\Psi_{JM_J, I, i, j, k}(\theta) = \mathcal{A} \left[[\psi_L(\theta) \chi_S^{\sigma_i}(4)]_{JM_J} \chi_I^{f_j} \chi_k^c \right], \quad (40)$$

where \mathcal{A} is the antisymmetry operator of doubly-heavy tetraquarks by considering the nature of identical particle interchange ($\bar{q}\bar{q}$, cc and bb). This is necessary for the

¹ The details on Gaussian parameters can be found in Ref. [82]

complete wave function of the 4-quark system is constructed from two sub-clusters, *i.e.* meson-meson and diquark-antidiquark structures. In particular, when the two heavy quarks are of the same flavor ($QQ = cc$ or bb), the definitions of these two configurations in Fig. 2 with the quark arrangements of $\bar{q}Q\bar{q}Q$ are both

$$\mathcal{A} = 1 - (13) - (24) + (13)(24). \quad (41)$$

However, due to the asymmetry between c - and b -quark, it is only two terms for $\bar{q}c\bar{q}b$ system and read as

$$\mathcal{A} = 1 - (13). \quad (42)$$

III. RESULTS

In the present work, we systematically investigate the low-lying S -wave states of $QQ\bar{q}\bar{q}$ ($q = u, c$ and $Q = c, b$) tetraquarks which both meson-meson and diquark-antidiquark configurations are considered. The parity for different doubly-heavy tetraquarks is positive under our assumption that the angular momenta l_1, l_2, l_3 , which appear in Eq. (32), are all 0. In this way, the total angular momentum, J , coincides with the total spin, S , and can take values of 0, 1 and 2. All possible dimeson and diquark-antidiquark channels for $cc\bar{q}\bar{q}$, $bb\bar{q}\bar{q}$ and $cb\bar{q}\bar{q}$ systems are listed in Table II, III and IV respectively, and they have been grouped according to total spin-pairity J^P and isospin I . For a clarity purpose, the third and fifth columns of these tables show the necessary basis combination in spin ($\chi_I^{\sigma_i}$), flavor ($\chi_I^{f_j}$), and color (χ_k^c) degrees-of-freedom. The physical channels with color-singlet (labeled with the superindex 1), hidden-color (labeled with the superindex 8) and diquark-antidiquark (labeled with $(QQ)(\bar{q}\bar{q})$) configurations are listed in the fourth and sixth columns.

Tables range from V to XVI summarized our calculated results (mass, size and component) of possible lowest-lying doubly-heavy tetraquarks. In particular, Tables VI, IX and XIV list each components of possible bound states of doubly-charm, doubly-bottom and charm-bottom tetraquarks in the complete coupled-channels calculation which all possible channels for a given quantum number IJ^P are considered. Their inner structures, the distance among any quark pair is shown in Tables VII, X and XV, this is in order to get some insight about either molecular or compact tetraquark we are dealing with. The rest tables below are of the calculated masses of these bound or resonance states of doubly-heavy tetraquarks, namely Tables V and VIII present the results of doubly-charm and doubly-bottom tetraquarks which quantum numbers are both of $I(J^P) = 0(1^+)$, and results on charm-bottom tetraquarks with $I(J^P) = 0(0^+)$, $0(1^+)$ and $0(2^+)$ are in Tables XI, XII and XIII respectively. Table XVI summarizes the obtained bound and resonance states of doubly-heavy tetraquarks in the complete coupled-channels calculation. Moreover, Fig. 3

to Fig. 7 present the distribution of complex energies of these doubly-heavy tetraquarks in coupled-channels calculation by complex scaling method. The transverse direction is of the real part of complex energy E , it stands for the mass of tetraquarks, and the longitudinal one is the imaginary part of E which is related to the width, $\Gamma = -2\text{Im}(E)$. However, the other quantum states of each doubly-heavy tetraquarks sectors do not appear here also have been considered in the calculation but neither bound nor resonance states are found.

In Tables V, VIII, XI, XII and XIII, the first column lists the physical channel of meson-meson and diquark-antidiquark (if it fulfills Pauli principle), and the experimental value of the noninteracting meson-meson threshold is also indicated in parenthesis; the second column refers to color-singlet (S), hidden-color (H) and coupled-channels (S+H) calculations for meson-meson configuration; the following two columns show the theoretical mass (M) and binding energy (E_B) of tetraquark state; moreover, as to avoid theoretical uncertainties coming from the quark model prediction of the meson spectra, the last column presents the re-scaled theoretical mass (M') of tetraquark state by attending to the corresponding experimental meson-meson threshold.

Now let us proceed to describe in detail our theoretical findings for each sector of doubly-heavy tetraquarks:

A. doubly-charm tetraquarks

In this sector, bound state and resonance are only found in the $I(J^P) = 0(1^+)$ state. Two possible meson-meson channels, D^+D^{*0} and $D^{*+}D^{*0}$, along with two diquark-antidiquark channels, $(cc)^*(\bar{u}\bar{d})$ and $(cc)(\bar{u}\bar{d})^*$ are studied in Table V. It is obviously to notice that there is no bound state in neither color-singlet (S) nor hidden-color channels (H) of the meson-meson configuration. However, this result is reversed by their coupled-channels calculation (S+H) and there are -1 MeV weakly binding energies both for D^+D^{*0} and $D^{*+}D^{*0}$ channels. After corrections, the re-scaled masses of these two channels are 3876 MeV and 4017 MeV, respectively. Meanwhile, the nature of molecular-type $D^{(*)+}D^{*0}$ structures are shown up since the color-singlet channels contributions are more than 95%.

In contrast to the weakly bound states around the $D^{(*)+}D^{*0}$ thresholds, there are almost -140 MeV binding energy for $(cc)^*(\bar{u}\bar{d})$ channel when compared with the theoretical threshold of D^+D^{*0} . However, the other diquark-antidiquark channel $(cc)(\bar{u}\bar{d})^*$ is above the D^+D^{*0} and $D^{*+}D^{*0}$ theoretical thresholds with $E_B = +305$ MeV and $+186$ MeV, respectively. This deeply bound diquark-antidiquark state $(cc)^*(\bar{u}\bar{d})$ motivates a further complete coupled-channels calculation which all the color-singlet, hidden-color of meson-meson channels and diquark-antidiquark ones are considered. The obtained mass is 3726 MeV which is 52 MeV lower than the single channel result of $(cc)^*(\bar{u}\bar{d})$, besides its nature of

TABLE II. All possible channels for $cc\bar{q}\bar{q}$ ($q = u$ or d) tetraquark systems.

J^P	Index	$I = 0$		$I = 1$	
		$\chi_J^{\sigma_i}; \chi_I^{f_j}; \chi_k^c$ [$i; j; k$]	Channel	$\chi_J^{\sigma_i}; \chi_I^{f_j}; \chi_k^c$ [$i; j; k$]	Channel
0^+	1	[1; 1; 1]	$(D^+ D^0)^1$	[1; 1; 1]	$(D^0 D^0)^1$
	2	[2; 1; 1]	$(D^{*+} D^{*0})^1$	[2; 1; 1]	$(D^{*0} D^{*0})^1$
	3	[1; 1; 2]	$(D^+ D^0)^8$	[1; 1; 2]	$(D^0 D^0)^8$
	4	[2; 1; 2]	$(D^{*+} D^{*0})^8$	[2; 1; 2]	$(D^{*0} D^{*0})^8$
	5			[3; 1; 4]	$(cc)(\bar{u}\bar{u})$
	6			[4; 1; 3]	$(cc)^*(\bar{u}\bar{u})^*$
1^+	1	[1; 1; 1]	$(D^+ D^{*0})^1$	[1; 1; 1]	$(D^0 D^{*0})^1$
	2	[3; 1; 1]	$(D^{*+} D^{*0})^1$	[3; 1; 1]	$(D^{*0} D^{*0})^1$
	3	[1; 1; 2]	$(D^+ D^{*0})^8$	[1; 1; 2]	$(D^0 D^{*0})^8$
	4	[3; 1; 2]	$(D^{*+} D^{*0})^8$	[3; 1; 2]	$(D^{*0} D^{*0})^8$
	5	[4; 1; 3]	$(cc)^*(\bar{u}\bar{d})$	[6; 1; 3]	$(cc)^*(\bar{u}\bar{u})^*$
	6	[5; 1; 4]	$(cc)(\bar{u}\bar{d})^*$		
2^+	1	[1; 1; 1]	$(D^{*+} D^{*0})^1$	[1; 1; 1]	$(D^{*0} D^{*0})^1$
	2	[1; 1; 2]	$(D^{*+} D^{*0})^8$	[1; 1; 2]	$(D^{*0} D^{*0})^8$
	3			[1; 1; 3]	$(cc)^*(\bar{u}\bar{u})^*$

TABLE III. All possible channels for $bb\bar{q}\bar{q}$ ($q = u$ or d) tetraquark systems.

J^P	Index	$I = 0$		$I = 1$	
		$\chi_J^{\sigma_i}; \chi_I^{f_j}; \chi_k^c$ [$i; j; k$]	Channel	$\chi_J^{\sigma_i}; \chi_I^{f_j}; \chi_k^c$ [$i; j; k$]	Channel
0^+	1	[1; 2; 1]	$(B^- \bar{B}^0)^1$	[1; 2; 1]	$(B^- B^-)^1$
	2	[2; 2; 1]	$(B^{*-} \bar{B}^{*0})^1$	[2; 2; 1]	$(B^{*-} B^{*-})^1$
	3	[1; 2; 2]	$(B^- \bar{B}^0)^8$	[1; 2; 2]	$(B^- B^-)^8$
	4	[2; 2; 2]	$(B^{*-} \bar{B}^{*0})^8$	[2; 2; 2]	$(B^{*-} B^{*-})^8$
	5			[3; 2; 4]	$(bb)(\bar{u}\bar{u})$
	6			[4; 2; 3]	$(bb)^*(\bar{u}\bar{u})^*$
1^+	1	[1; 2; 1]	$(B^- \bar{B}^{*0})^1$	[1; 2; 1]	$(B^- B^{*-})^1$
	2	[3; 2; 1]	$(B^{*-} \bar{B}^{*0})^1$	[3; 2; 1]	$(B^{*-} B^{*-})^1$
	3	[1; 2; 2]	$(B^- \bar{B}^{*0})^8$	[1; 2; 2]	$(B^- B^{*-})^8$
	4	[3; 2; 2]	$(B^{*-} \bar{B}^{*0})^8$	[3; 2; 2]	$(B^{*-} B^{*-})^8$
	5	[4; 2; 3]	$(bb)^*(\bar{u}\bar{d})$	[6; 2; 3]	$(bb)^*(\bar{u}\bar{u})^*$
	6	[5; 2; 4]	$(bb)(\bar{u}\bar{d})^*$		
2^+	1	[1; 2; 1]	$(B^{*-} \bar{B}^{*0})^1$	[1; 2; 1]	$(B^{*-} B^{*-})^1$
	2	[1; 2; 2]	$(B^{*-} \bar{B}^{*0})^8$	[1; 2; 2]	$(B^{*-} B^{*-})^8$
	3			[1; 2; 3]	$(bb)^*(\bar{u}\bar{u})^*$

compact doubly-charm tetraquark state is clearly presented in Table VII where the distance between any two quarks are calculated and the obtained size of this four-quark system is less than 0.67 fm. Table VI shows each

component in the coupled-channels calculation. In particular, two mainly comparable components, color-singlet channel $D^+ D^{*0}$ (25.8%) and $(cc)^*(\bar{q}\bar{q})$ one (36.7%), consist with our result of strong coupling effect and compact

TABLE IV. All possible channels for $cb\bar{q}\bar{q}$ ($q = u$ or d) tetraquark systems. For a brief purpose, only the $D^{(*)0}B^{(*)0}$ structures are listed and the corresponding $D^{(*)+}\bar{B}^{(*)-}$ ones are absent in $I = 0$. However, all these configurations are still employed in constructing the wavefunctions of 4-quark systems.

J^P	Index	$I = 0$		$I = 1$	
		$\chi_J^{\sigma_i}; \chi_I^{f_j}; \chi_k^c$ [$i; j; k$]	Channel	$\chi_J^{\sigma_i}; \chi_I^{f_j}; \chi_k^c$ [$i; j; k$]	Channel
0^+	1	[1; 3; 1]	$(D^0\bar{B}^0)^1$	[1; 3; 1]	$(D^0B^-)^1$
	2	[2; 3; 1]	$(D^{*0}\bar{B}^{*0})^1$	[2; 3; 1]	$(D^{*0}B^{*-})^1$
	3	[1; 3; 2]	$(D^0\bar{B}^0)^8$	[1; 3; 2]	$(D^0B^-)^8$
	4	[2; 3; 2]	$(D^{*0}\bar{B}^{*0})^8$	[2; 3; 2]	$(D^{*0}B^{*-})^8$
	5	[3; 3; 3]	$(cb)(\bar{u}\bar{d})$	[3; 3; 4]	$(cb)(\bar{u}\bar{u})$
	6	[4; 3; 4]	$(cb)^*(\bar{u}\bar{d})^*$	[4; 3; 3]	$(cb)^*(\bar{u}\bar{u})^*$
1^+	1	[1; 3; 1]	$(D^0\bar{B}^{*0})^1$	[1; 3; 1]	$(D^0B^{*-})^1$
	2	[2; 3; 1]	$(D^{*0}\bar{B}^0)^1$	[2; 3; 1]	$(D^{*0}B^-)^1$
	3	[3; 3; 1]	$(D^{*0}\bar{B}^{*0})^1$	[3; 3; 1]	$(D^{*0}B^{*-})^1$
	4	[1; 3; 2]	$(D^0\bar{B}^{*0})^8$	[1; 3; 2]	$(D^0B^{*-})^8$
	5	[2; 3; 2]	$(D^{*0}\bar{B}^0)^8$	[2; 3; 2]	$(D^{*0}B^-)^8$
	6	[3; 3; 2]	$(D^{*0}\bar{B}^{*0})^8$	[3; 3; 2]	$(D^{*0}B^{*-})^8$
	7	[4; 3; 3]	$(cb)^*(\bar{u}\bar{d})$	[4; 3; 4]	$(cb)^*(\bar{u}\bar{u})$
	8	[5; 3; 4]	$(cb)(\bar{u}\bar{d})^*$	[5; 3; 3]	$(cb)(\bar{u}\bar{u})^*$
	9	[6; 3; 4]	$(cb)^*(\bar{u}\bar{d})^*$	[6; 3; 3]	$(cb)^*(\bar{u}\bar{u})^*$
2^+	1	[1; 3; 1]	$(D^{*0}\bar{B}^{*0})^1$	[1; 3; 1]	$(D^{*0}B^{*-})^1$
	2	[1; 3; 2]	$(D^{*0}\bar{B}^{*0})^8$	[1; 3; 2]	$(D^{*0}B^{*-})^8$
	3	[1; 3; 4]	$(cb)^*(\bar{u}\bar{d})^*$	[1; 3; 3]	$(cb)^*(\bar{u}\bar{u})^*$

TABLE V. Lowest-lying states of doubly-charm tetraquarks with quantum numbers $I(J^P) = 0(1^+)$, unit in MeV.

Channel	Color	M	E_B	M'
D^+D^{*0} (3877)	S	3915	0	3877
	H	4421	+506	4383
	S+H	3914	-1	3876
Percentage (S;H): 97.3%; 2.7%				
$D^{*+}D^{*0}$ (4018)	S	4034	0	4018
	H	4390	+356	4374
	S+H	4033	-1	4017
Percentage (S;H): 95.5%; 4.5%				
$(cc)^*(\bar{u}\bar{d})$		3778		
$(cc)(\bar{u}\bar{d})^*$		4220		
Mixed		3726		

tetraquark structure.

The obtained deeply bound doubly-charm tetraquark with $M = 3726$ MeV by CSM in the complete coupled

TABLE VI. Component of each channel in coupled-channels calculation with $IJ^P = 01^+$, the numbers 1 and 8 of superscript are for singlet-color and hidden-color channel respectively.

$(D^+D^{*0})^1$	$(D^{*+}D^{*0})^1$	$(D^+D^{*0})^8$	$(D^{*+}D^{*0})^8$
25.8%	15.4%	10.7%	11.2%
$(cc)^*(\bar{u}\bar{d})$	$(cc)(\bar{u}\bar{d})^*$		
36.7%	0.2%		

TABLE VII. The distance, in fm, between any two quarks of the found tetraquark bound-states in coupled-channels calculation ($q = u, d$).

$r_{\bar{u}\bar{d}}$	$r_{\bar{q}c}$	r_{cc}
0.658	0.666	0.522

channels calculation is clearly shown in Fig. 3. We vary the rotated angle θ from 0° to 6° , and this bound state remains on the real-axis. Particularly, the black dots in the real-axis are the calculated masses in coupled-channels calculation with $\theta = 0^\circ$, and the red, blue and green

ones are for complex energies with $\theta = 2^\circ, 4^\circ$ and 6° , respectively. Generally, they are aligned along the threshold lines with the same color and the nature of scattering state of D^+D^{*0} and $D^{*+}D^{*0}$ in coupled-channels is clearly for their calculated poles always move along the cut lines when the scaling angle θ changes. However, there is a mismatch between the calculated dots and threshold lines in high energy region with large width. Nevertheless, we mainly focus on the low-lying state in this work and those calculation noises still present a nature of scattering states with obviously moving track.

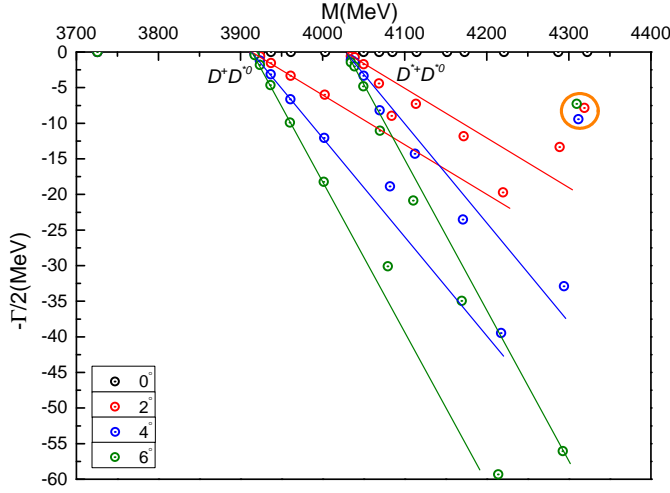


FIG. 3. Complex energies of doubly-charm tetraquarks with $IJ^P = 01^+$ in the coupled channels calculation, θ varying from 0° to 6° .

In Fig. 3 one can see that there is a possible resonance pole marked with orange circle above the nearer $D^{*+}D^{*0}$ threshold lines. The three dots obtained by the CSM calculation with $\theta = 2^\circ, 4^\circ$ and 6° , respectively are located in a quite small energy region. Their complex energies are listed in Table XVI and the estimated resonance mass and width is ~ 4312 MeV and ~ 16 MeV, respectively. By considering the fact that the resonance pole is near $D^{*+}D^{*0}$ threshold lines than D^+D^{*0} , hence the former channel should play a more important role in this resonance state.

B. doubly-bottom tetraquarks

We herein investigate $B^{(*)}-\bar{B}^{*0}$ and $(bb)^*(\bar{u}\bar{d})^{(*)}$ channels which are similar to the doubly-charm tetraquarks. Possible bound and resonance states are also obtained only in $I(J^P) = 0(1^+)$ state. However, with much more heavier b -flavored quarks included, possible bound states of color-singlet channels of $B^-\bar{B}^{*0}$ and $B^{*-}\bar{B}^{*0}$ are found, their binding energies are -12 MeV and -11 MeV respectively. Additionally, in Table VIII one can find that nearly triple binding energies are obtained both for $B^-\bar{B}^{*0}$ ($E_B = -35$ MeV) and $B^{*-}\bar{B}^{*0}$

TABLE VIII. Lowest-lying states of doubly-bottom tetraquarks with quantum numbers $I(J^P) = 0(1^+)$, unit in MeV.

Channel	Color	M	E_B	M'
$B^-\bar{B}^{*0}$ (10604)	S	10585	-12	10592
	H	10987	+390	10994
	S+H	10562	-35	10569
Percentage (S;H): 83.0%; 17.0%				
$B^{*-}\bar{B}^{*0}$ (10650)	S	10627	-11	10639
	H	10974	+336	10986
	S+H	10601	-37	10613
Percentage (S;H): 79.6%; 20.4%				
$(bb)^*(\bar{u}\bar{d})$		10261		
$(bb)(\bar{u}\bar{d})^*$		10787		
Mixed		10238 ^{1st}		
		10524 ^{2nd}		

TABLE IX. Component of each channel in coupled-channels calculation with $IJ^P = 01^+$, the numbers 1 and 8 of superscript are for singlet-color and hidden-color channel respectively.

	$(B^-\bar{B}^{*0})^1$	$(B^{*-}\bar{B}^{*0})^1$	$(B^-\bar{B}^{*0})^8$
1st	20.7%	17.9%	9.3%
2nd	25.6%	14.8%	9.5%
	$(B^{*-}\bar{B}^{*0})^8$	$(bb)^*(\bar{u}\bar{d})$	$(bb)(\bar{u}\bar{d})^*$
1st	9.4%	42.6%	0.1%
2nd	9.1%	40.2%	0.8%

TABLE X. The distance, in fm, between any two quarks of the found tetraquark bound-states in coupled-channels calculation, ($q = u, d$).

	$r_{\bar{u}\bar{d}}$	$r_{\bar{q}b}$	r_{bb}
1st	0.604	0.608	0.328
2nd	0.830	0.734	0.711

($E_B = -37$ MeV) when the hidden-color channels are incorporated in the calculation. These deeper bound states than $D^{(*)+}D^{*0}$ cases also indicate a strong coupling which is about 80% color-singlet component for $B^{(*)}-\bar{B}^{*0}$. After a mass shift for these two bound states, the slightly modified masses of doubly-bottom tetraquarks are 10569 MeV and 10613 MeV respectively.

In diquark-antidiquark configuration, according to the $B^-\bar{B}^{*0}$ theoretical thresholds, one tightly bound state of $(bb)^*(\bar{u}\bar{d})$ whose binding energy is $E_B = -336$ MeV and one excited state of $(bb)(\bar{u}\bar{d})^*$ with $E_B = +190$ MeV

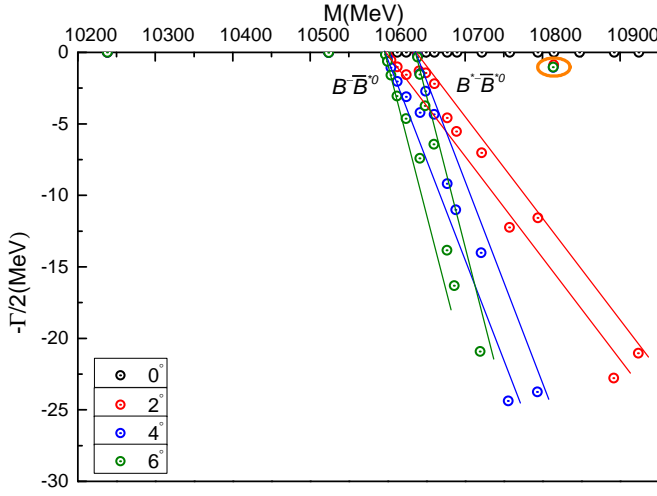


FIG. 4. Complex energies of doubly-bottom tetraquarks with $I(J^P) = 0(1^+)$ in the coupled channels calculation, θ varying from 0° to 6° .

are shown in Table VIII, respectively. This situation is also consistent with $(cc)^*(\bar{u}\bar{d})^{(*)}$ channels which are of smaller binding energies. The obtained deeply bound state $(bb)^*(\bar{u}\bar{d})$ at 10261 MeV is supported by Refs. [52, 53, 55, 56], only ~ 130 MeV lower than the predicted mass in Ref. [53].

Furthermore, two bound states are found in a coupled-channels calculation which all the channels listed in Table VIII are considered, their masses are 10238 MeV and 10524 MeV, respectively. Clearly, the $(bb)^*(\bar{u}\bar{d})$ diquark-antidiquark channel is pushed down by 23 MeV due to the coupling effect, and the second bound state ($M = 10524$ MeV) is 73 MeV below the $B^- \bar{B}^{*0}$ theoretical threshold. Then with a purpose of disentangling the nature of these two obtained bound states, their components and inner structures are studied. One can see in Table IX that the components of the two bound states are quite comparable and both about 42% for $(bb)^*(\bar{u}\bar{d})$ channel and about 20% sub-dominant for the color-singlet channel of $B^{(*)-} \bar{B}^{*0}$. With no more than 0.83 fm distance for any quark pair listed in Table X, the compact tetraquark structures for these two bound states are clearly presented again, and one need to mention that the distances of two bottom quarks for them are only 0.328 fm and 0.711 fm, respectively.

In Table XVI and Fig. 4 one can find that the two bound states are stable against the change of scaling angle θ . Besides, one resonance state which mass and width is 10814 MeV and 2 MeV, respectively is obtained in the complete coupled-channels calculation with various rotated angle θ . We mark it with a big orange circle where the three dots are almost overlap and their complex energies within θ taken the value of 2° , 4° and 6° are listed in Table XVI, respectively. This narrow width resonance pole is close to $B^{*-} \bar{B}^{*0}$ threshold line and more contributions should be made by this channel. However, the

TABLE XI. Lowest-lying states of charm-bottom tetraquarks with quantum numbers $I(J^P) = 0(0^+)$, unit in MeV.

Channel	Color	M	E_B	M'
$D^0 \bar{B}^0$ (7147)	S	7172	-4	7143
	H	7685	+509	7656
	S+H	7171	-5	7142
Percentage (S;H): 96.4%; 3.6%				
$D^{*0} \bar{B}^{*0}$ (7334)	S	7327	-9	7325
	H	7586	+250	7584
	S+H	7297	-39	7295
Percentage (S;H): 87.8%; 12.2%				
$(cb)(\bar{u}\bar{d})$		7028		
$(cb)^*(\bar{u}\bar{d})^*$		7482		
Mixed		6980		

other poles with a scattering nature are generally aligned along the $B^- \bar{B}^{*0}$ and $B^{*-} \bar{B}^{*0}$ threshold lines.

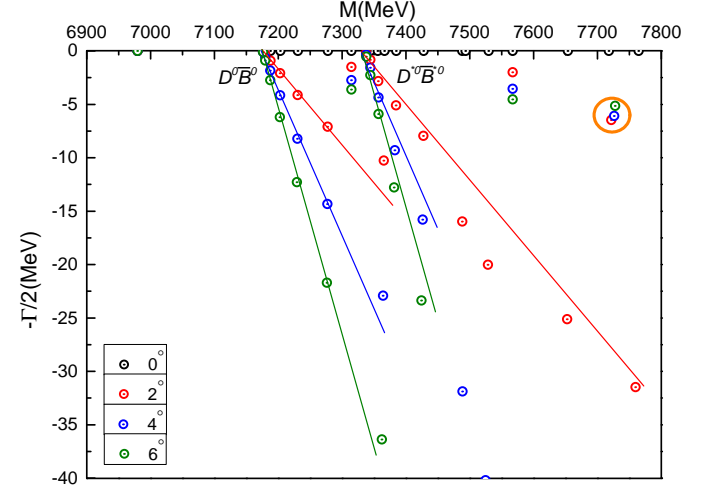


FIG. 5. Complex energies of charm-bottom tetraquarks with $I(J^P) = 0(0^+)$ in the coupled channels calculation, θ varying from 0° to 6° .

C. charm-bottom tetraquarks

In these sector, some bound or resonance states are obtained only for iso-scalar tetraquarks, and our theoretical findings in meson-meson channels are comparable with those results in Table V of Ref. [94]. Hence we will discuss them according to $I(J^P)$ quantum numbers individually.

The $I(J^P) = 0(0^+)$ channel: Loosely bound states of the color-singlet channel of $D^0 \bar{B}^0$ and $D^{*0} \bar{B}^{*0}$ are

found, their binding energies are -4 MeV and -9 MeV, respectively. In Table XI one can realize that there is only a remarkable coupling effect ($E_B = -39$ MeV) on $D^{*0}\bar{B}^{*0}$ configuration when the hidden-color channel is incorporated, and almost no influence on $D^0\bar{B}^0$ channel with only 1 MeV binding energy increased. This is supported by our calculated proportion for color-singlet and hidden-color channels: 96.4% for $(D^0\bar{B}^0)^1$ and 87.8% for $(D^{*0}\bar{B}^{*0})^1$. Meanwhile, one deeply bound state $(cb)(\bar{u}\bar{d})$ with $E_B = -148$ MeV and one excited state $(cb)^*(\bar{u}\bar{d})^*$ with $E_B = +306$ MeV are found with respect to the $D^0\bar{B}^0$ theoretical threshold. The binding energy of lowest-lying state is increased by 48 MeV in the complete coupled-channels calculation. This tightly bound state which mass is 6980 MeV brings us a compact doubly-heavy tetraquark structure again, Table XV presents the size of state around 0.6 fm and even smaller distance, 0.428 fm for cb quark pair. All of these features can be related to the strong coupling effect which almost 50% for $(cb)(\bar{u}\bar{d})$, 26.4% for $(D^0\bar{B}^0)^1$ and 21.5% for $(D^{*0}\bar{B}^{*0})^1$ channels are shown in Table XIV.

In the complex scaling computation that the investigated region of rotated angle θ is the same as previous two types of tetraquark states, the bound state along with a resonance are presented in Fig. 5. Specifically, four dots whose θ taken the value of 0° , 2° , 4° and 6° , respectively are overlap exactly at mass is 6980 MeV on the real-axis. The resonance pole is found near the mass of 7726 MeV and its width is ~ 12 MeV according to Table XVI. Moreover, one can find in Fig. 5 that the resonance state is far from the $D^0\bar{B}^0$ threshold and accordingly, the majority contributions should owing to $D^{*0}\bar{B}^{*0}$ channel.

The rest calculated poles in Fig. 5 are basically fit well with the $D^0\bar{B}^0$ and $D^{*0}\bar{B}^{*0}$ threshold lines, except for two cases. Namely, the dots always descend slowly with the increasing of scaling angle θ both at mass is 7314 MeV and 7567 MeV. They can not be identified as resonance states due to the instability.

The $I(J^P) = 0(1^+)$ channel: Both of three channels in meson-meson $D^{(*)0}\bar{B}^{(*)0}$ and diquark-antidiquark $(cb)^{(*)}(\bar{u}\bar{d})^{(*)}$ configurations are studied in Table XII. Four similar features as the other doubly-heavy tetraquarks discussed before can be drawn: (i) loosely bound states with $E_B = -3$ MeV, -2 MeV and -2 MeV for the three color-singlet channels of $D^0\bar{B}^{*0}$, $D^{*0}\bar{B}^0$ and $D^{*0}\bar{B}^{*0}$ respectively, (ii) the coupling between color-singlet and hidden-color channels are quite weak (E_B increased by 1 MeV) for $D^0\bar{B}^{*0}$ and $D^{*0}\bar{B}^0$ configurations, but 8 MeV increased binding energy for $D^{*0}\bar{B}^{*0}$, (iii) only one deeply bound state in single channel calculation, namely $E_B = -178$ MeV for $(cb)^*(\bar{u}\bar{d})$ channel when compared with the lowest theoretical threshold of $D^0\bar{B}^{*0}$, and (iv) more tightly bound state which mass is 6997 MeV in the complete coupled-channels calculation.

In Table XIV one can see that the most contribution 46.4% comes from $(cb)^*(\bar{u}\bar{d})$ channel and other three sub-dominant channels are 20.2% for $(D^0\bar{B}^{*0})^1$, 11.6%

TABLE XII. Lowest-lying states of charm-bottom tetraquarks with quantum numbers $I(J^P) = 0(1^+)$, unit in MeV.

Channel	Color	M	E_B	M'
$D^0\bar{B}^{*0}$ (7193)	S	7214	-3	7190
	H	7694	+477	7670
	S+H	7213	-4	7189
Percentage (S;H): 96.8%; 3.2%				
$D^{*0}\bar{B}^0$ (7288)	S	7293	-2	7286
	H	7707	+412	7700
	S+H	7292	-3	7285
Percentage (S;H): 96.8%; 3.2%				
$D^{*0}\bar{B}^{*0}$ (7334)	S	7334	-2	7332
	H	7691	+354	7688
	S+H	7326	-10	7324
Percentage (S;H): 89.3%; 10.7%				
$(cb)^*(\bar{u}\bar{d})$		7039		
$(cb)(\bar{u}\bar{d})^*$		7531		
$(cb)^*(\bar{u}\bar{d})^*$		7507		
Mixed		6997		

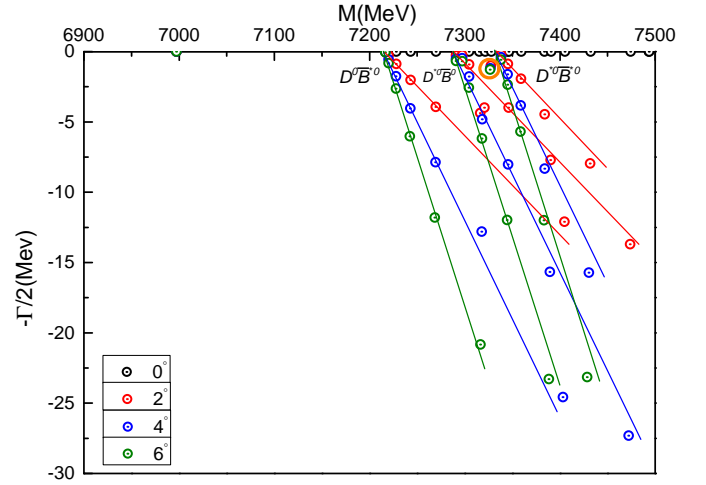


FIG. 6. Complex energies of charm-bottom tetraquarks with $I(J^P) = 0(1^+)$ in the coupled channels calculation, θ varying from 0° to 6° .

for $(D^{*0}\bar{B}^0)^1$ and 16.8% for $(D^{*0}\bar{B}^{*0})^1$. These facts of strong coupling effect along with the domination of diquark-antidiquark configuration result in a compact structure again, and one can find a comparable size between $I(J^P) = 0(1^+)$ and $0(0^+)$ state in Table XV.

Fig. 6 presents the distribution of complex energies in the complete coupled-channels calculation. Three scattering states of $D^0\bar{B}^{*0}$, $D^{*0}\bar{B}^0$ and $D^{*0}\bar{B}^{*0}$ are clearly

TABLE XIII. Lowest-lying states of charm-bottom tetraquarks with quantum numbers $I(J^P) = 0(2^+)$, unit in MeV.

Channel	Color	M	E_B	M'
$D^{*0}\bar{B}^{*0}$	S	7334	-2	7332
(7334)	H	7720	+384	7718
	S+H	7334	-2	7332
Percentage (S;H): 99.8%; 0.2%				
$(cb)^*(\bar{u}\bar{d})^*$		7552		
Mixed		7333		

shown and the bound state which mass is 6997 MeV remains on the real-axis. Meanwhile, one narrow width resonance state as doubly-bottom tetraquarks whose $\Gamma = 2$ MeV is obtained and marked with a orange circle in the figure. $D^{*0}\bar{B}^0$ and $D^{*0}\bar{B}^{*0}$ channels should be both important to this quite narrow resonance pole which is among the threshold lines of them. The resonance mass is 7327 MeV and its width is ~ 2.4 MeV in the CSM computation with θ varying from 0° to 6° in Table XVI.

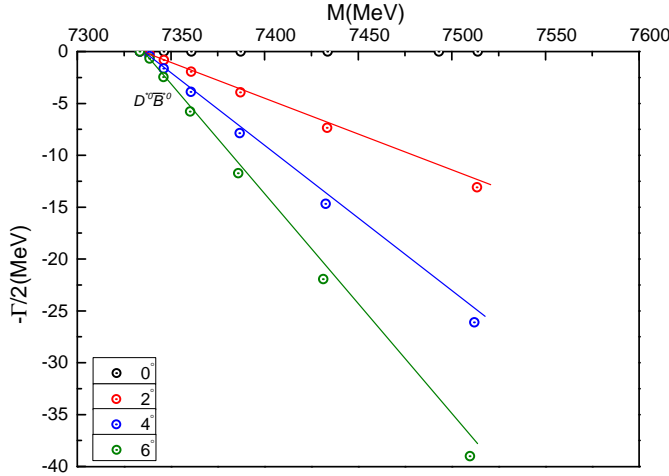


FIG. 7. Complex energies of charm-bottom tetraquarks with $I(J^P) = 0(2^+)$ in the coupled channels calculation, θ varying from 0° to 6° .

The $I(J^P) = 0(2^+)$ channel: Only two channels contribute to this case: $D^{*0}\bar{B}^{*0}$ meson-meson channel and diquark-antidiquark one $(cb)^*(\bar{u}\bar{d})^*$. As in all cases studied before, a loosely bound state of color-singlet channel $D^{*0}\bar{B}^{*0}$ is obtained with $E_B = -2$ MeV. Furthermore, the coupling is still quite weak in the complete coupled-channels investigation for $(D^{*0}\bar{B}^{*0})^1$ channel contributes 98.6%, and the calculated mass is 7333 MeV which is quite close to the color-singlet channel one of 7334 MeV. This indicates the nature of molecular-type meson-meson structure and it is also consistent with the obtained size in Table XV where the distances be-

TABLE XIV. Component of each channel in coupled-channels calculation, the numbers 1 and 8 of superscript are for singlet-color and hidden-color channel respectively, ($q = u, d$).

IJ^P	$(D^0\bar{B}^0)^1$	$(D^{*0}\bar{B}^{*0})^1$	$(D^0\bar{B}^0)^8$	$(D^{*0}\bar{B}^{*0})^8$
00^+	26.4%	21.5%	1.6%	1.9%
	$(cb)(\bar{u}\bar{d})$	$(cb)^*(\bar{u}\bar{d})^*$		
	48.5%	0.1%		
01^+	$(D^0\bar{B}^{*0})^1$	$(D^{*0}\bar{B}^0)^1$	$(D^{*0}\bar{B}^{*0})^1$	$(D^0\bar{B}^{*0})^8$
	20.2%	11.6%	16.8%	1.4%
	$(D^{*0}\bar{B}^0)^8$	$(D^{*0}\bar{B}^{*0})^8$	$(cb)^*(\bar{u}\bar{d})$	$(cb)(\bar{u}\bar{d})^*$
	1.3%	1.8%	46.4%	0.1%
	$(cb)^*(\bar{u}\bar{d})^*$			
	0.4%			
02^+	$(D^{*0}\bar{B}^{*0})^1$	$(D^{*0}\bar{B}^{*0})^8$	$(cb)^*(\bar{u}\bar{d})^*$	
	98.6%	0.3%	1.1%	

TABLE XV. The distance, in fm, between any two quarks of the found tetraquark bound-states in coupled-channels calculation, ($q = u, d$).

IJ^P	$r_{\bar{u}\bar{d}}$	$r_{\bar{q}c}$	$r_{\bar{q}b}$	r_{cb}
00^+	0.635	0.653	0.610	0.428
01^+	0.632	0.661	0.616	0.434
02^+	2.248	1.612	1.597	2.102

tween any two quarks are about $1.6 \text{ fm} \sim 2.2 \text{ fm}$.

In additional, no resonance state is found in the complete coupled-channels calculation with θ varying from 0° to 6° . The loosely bound state with $M = 7333$ MeV and another scattering state of $D^{*0}\bar{B}^{*0}$ are presented in Fig. 7, respectively.

IV. EPILOGUE

In a complex scaling range of chiral quark formalism, by considering meson-meson and diquark-antidiquark configurations along with all color structures (couplings are also considered), *i.e.* color-singlet and hidden-color channels for dimeson structure; color triplet-antitriplet and sextet-antisextet channels for $(QQ)(\bar{q}\bar{q})$ structure, we have studied the possibility of having tetraquark bound- and resonance-states in the doubly-heavy sectors with quantum numbers $J^P = 0^+, 1^+$ and 2^+ , and in the 0 and 1 isospin sectors. For possible bound states in the complete coupled-channels study, their inner structures and components are also analyzed by computing the distances among any pair of quarks and the contri-

TABLE XVI. Possible bound and resonance states for $QQ\bar{q}\bar{q}$ ($q = u$ or d) tetraquarks in CSM with rotated angle θ varying from 0° to 6° . The imaginary part of complex energy and resonance width are with the relation of $\text{Im}(E) = -\Gamma/2$, unit in MeV.

		0°	2°	4°	6°
$cc\bar{q}\bar{q}$	bound state	3726	3726	3726	3726
$IJ^P = 01^+$	resonance state	-	$4319 - 7.9i$	$4312 - 9.4i$	$4310 - 7.3i$
$bb\bar{q}\bar{q}$	bound state	10238; 10524	10238; 10524	10238; 10524	10238; 10524
$IJ^P = 01^+$	resonance state	-	$10814 - 0.9i$	$10814 - 1.1i$	$10814 - 1.0i$
$cb\bar{q}\bar{q}$	bound state	6980	6980	6980	6980
$IJ^P = 00^+$	resonance state	-	$7722 - 6.5i$	$7726 - 6.1i$	$7728 - 5.2i$
$cb\bar{q}\bar{q}$	bound state	6997	6997	6997	6997
$IJ^P = 01^+$	resonance state	-	$7327 - 1.0i$	$7327 - 1.2i$	$7327 - 1.3i$
$cb\bar{q}\bar{q}$	bound state	7333	7333	7333	7333
$IJ^P = 02^+$	resonance state	-	-	-	-

butions of each channel's wave functions. Masses and widths for possible resonance states are also calculated in the coupled-channels calculation. The model parameters which are included in the perturbative one-gluon exchange, the nonperturbative linear-screened confining and Goldstone-boson exchange interactions between light quarks have been fitted in the past through hadron, hadron-hadron and multi-quark phenomenology.

For all quantum states of the investigated doubly-heavy tetraquarks, $cc\bar{q}\bar{q}$, $bb\bar{q}\bar{q}$ and $cb\bar{q}\bar{q}$ ($q = u, d$), tightly bound and narrow resonance states are only obtained in $IJ^P = 01^+$ state for the former two sectors, and they are also obtained for $cb\bar{q}\bar{q}$ in 00^+ and 01^+ states. However, only loosely bound state is found for charm-bottom tetraquarks in 02^+ states. All of these states within meson-meson configurations are loosely bound whether in color-singlet channels or coupling to hidden-color ones. However, compact structures are available in diquark-antidiquark channels except for charm-bottom tetraquarks in 02^+ states. Let us characterize the features in detail.

Firstly, in doubly-charm tetraquark states, two loosely bound states D^+D^{*0} and $D^{*+}D^{*0}$ with mass 3876 MeV and 4017 MeV, respectively are obtained in $IJ^P = 01^+$ state. Meanwhile, a deeply bound state with $(cc)^*(\bar{u}\bar{d})$ diquark-antidiquark structure is found at 3778 MeV. In the complete coupled-channels calculation the lowest-lying state mass is 3726 MeV, and the compact tetraquark states size is 0.52 – 0.66 fm. Meanwhile, a resonance state which is mainly induced by $D^{*+}D^{*0}$ channel is obtained and the estimated mass and width is 4312 MeV and 16 MeV, respectively.

Secondly, similar to the doubly-charm tetraquarks, we found loosely bound states of $B^-\bar{B}^{*0}$ and $B^{*-}\bar{B}^{*0}$ with $IJ^P = 01^+$, the predicted masses are 10569 MeV and 10613 MeV, respectively. There are $\sim 20\%$ contributions from hidden-color channels for these two molecular

states. Diquark-antidiquark state $(bb)^*(\bar{u}\bar{d})$ is much more tightly bound with a binding energy $E_B = -336$ MeV when compares with the theoretical threshold of $B^-\bar{B}^{*0}$ channel. In the complete coupled-channels calculation, two compact tetraquark bound states with mass at 10238 MeV and 10524 MeV, respectively are obtained. The distances among any quark pair of them are less than 0.83 fm. Besides, a narrow resonance state with mass $M = 10814$ MeV and width $\Gamma = 2$ MeV is found, and $B^{*-}\bar{B}^{*0}$ channel plays an important role to this state.

In additional, possible charm-bottom tetraquark states are found in three quantum states $IJ^P = 00^+$, 01^+ and 02^+ . Specifically, in 00^+ state, $D^0\bar{B}^0(7142)$ and $D^{*0}\bar{B}^{*0}(7295)$; in 01^+ state, $D^0\bar{B}^{*0}(7189)$, $D^{*0}\bar{B}^0(7285)$ and $D^{*0}\bar{B}^{*0}(7324)$; and in 02^+ state, $D^{*0}\bar{B}^{*0}(7332)$, the predicted masses for these molecular states are correspondingly signed in the brackets. The compact tetraquarks $(cb)(\bar{u}\bar{d})$ and $(cb)^*(\bar{u}\bar{d})$ with mass at 7028 MeV and 7039 MeV are found in 00^+ and 01^+ states, respectively. In the complete coupled-channels calculation, these two states are of lower masses 6980 MeV and 6997 MeV, besides their size are both less than 0.67 fm. However, 02^+ state remains the molecular type structure due to quite weak coupling. Two resonances are available for 00^+ and 01^+ states, their mass and width are 7726 MeV, 12 MeV and 7327 MeV, 2.4 MeV, respectively. $D^{*0}\bar{B}^{*0}$ channel is crucial for the resonance state with $IJ^P = 00^+$ and resonance in 01^+ state is mainly induced by $D^{*0}\bar{B}^0$ and $D^{*0}\bar{B}^{*0}$ channels.

Finally, our results in this work by the phenomenological framework of chiral quark model are expecting to be confirmed in future high energy experiments. Meanwhile, a natural extension of our investigation in next step will be the other open-heavy tetraquark states, *i.e.* $QQ\bar{Q}\bar{q}$ systems. Properties in those almost non-relativistic systems are also absorbing.

ACKNOWLEDGMENTS

G. Yang would like to thank L. He for his support and informative discussions. Work partially financed

by: China Postdoctoral Science Foundation Grant no. 2019M650617; National Natural Science Foundation of China under Grant nos. 11535005 and 11775118; Spanish Ministerio de Economía, Industria y Competitividad under contract no. FPA2017-86380-P.

-
- [1] S. K. Choi *et al.* (LEPS Collaboration), Phys. Rev. Lett. **91**, 262001 (2003).
 - [2] D. Acosta *et al.* (CDF II Collaboration), Phys. Rev. Lett. **93**, 072001 (2004).
 - [3] V. M. Abazov *et al.* (D0 Collaboration), Phys. Rev. Lett. **93**, 162002 (2004).
 - [4] B. Aubert *et al.* (BABAR Collaboration), Phys. Rev. D **71**, 071103 (2005).
 - [5] S. Godfrey and N. Isgur, Phys. Rev. D **32**, 189 (1985).
 - [6] D. Ebert, R. N. Faustov and V. O. Galkin, Eur. Phys. J. C **71**, 1825 (2011).
 - [7] J. Segovia, D. R. Entem, F. Fernandez and E. Hernandez, Int. J. Mod. Phys. **E22**, 1330026 (2013).
 - [8] J. Vijande, F. Fernandez and A. Valcarce, J. Phys. **G31**, 481 (2005).
 - [9] T. Barnes and S. Godfrey, Phys. Rev. D **69**, 054008 (2004).
 - [10] E. J. Eichten, K. Lane and C. Quigg, Phys. Rev. D **69**, 094019 (2004).
 - [11] Y. Dong, A. Faessler, T. Gutsche and V. E. Lyubovitskij, Phys. Rev. D **77**, 094013 (2008).
 - [12] Y. Dong, A. Faessler, T. Gutsche, S. Kovalenko and V. E. Lyubovitskij, Phys. Rev. D **79**, 094013 (2009).
 - [13] D. Gamermann, J. Nieves, E. Oset and E. R. Arriola, Phys. Rev. D **81**, 014029 (2010).
 - [14] F. -K. Guo, C. Hanhart, Y. S. Kalashnikova, U. -G. Meissner and A. V. Nefediev, Phys. Lett. B **742**, 394 (2015).
 - [15] L. Maiani, F. Piccinini, A. D. Polosa and V. Riquer, Phys. Rev. D **71**, 014028 (2005).
 - [16] P. G. Ortega, J. Segovia, D. R. Entem and F. Fernández, Phys. Rev. D **81**, 054023 (2010).
 - [17] S. Coito, G. Rupp and E. Beveren, Eur. Phys. J. C **71**, 1762 (2011).
 - [18] J. Ferretti and G. Galatà, Phys. Rev. D **90**, 054010 (2014).
 - [19] M. Cardoso, G. Rupp and E. Beveren, Eur. Phys. J. C **75**, 26 (2015).
 - [20] Y. Tan and J. Ping, Phys. Rev. D **100**, 034022 (2019).
 - [21] B. Aubert *et al.* (BABAR Collaboration), Phys. Rev. Lett. **95**, 142001 (2005).
 - [22] S. -K. Choi *et al.* (Belle Collaboration), Phys. Rev. Lett. **100**, 142001 (2008).
 - [23] T. Aaltonen *et al.* (CDF Collaboration), Phys. Rev. Lett. **102**, 242002 (2009).
 - [24] M. Ablikim *et al.* (BESIII Collaboration), Phys. Rev. Lett. **110**, 252001 (2013).
 - [25] R. Aaij *et al.* (LHCb Collaboration), Phys. Rev. Lett. **115**, 072001 (2015).
 - [26] R. Aaij *et al.* (LHCb Collaboration), Phys. Rev. Lett. **122**, 222001 (2019).
 - [27] H. -X. Chen, W. Chen, X. Liu and S. -L. Zhu, Phys. Rep. **639**, 1 (2016).
 - [28] H. -X. Chen, W. Chen, X. Liu, Y. -R. Liu and S. -L. Zhu, Rep. Prog. Phys. **80**, 076201 (2017).
 - [29] F. -K. Guo, C. Hanhart, U. -G. Meissner, Q. Wang, Q. Zhao and B. -S. Zou, Rev. Mod. Phys. **90**, 015004 (2018).
 - [30] S. L. Olsen, T. Skwarnicki and D. Zieminska, Rev. Mod. Phys. **90**, 015003 (2018).
 - [31] V. Khachatryan *et al.* (CMS Collaboration), J. High Energ. Phys. **05**, 013 (2017).
 - [32] L. C. Bland *et al.* (A_N DY Collaboration), arXiv: 1909.03124 [nucl-ex].
 - [33] R. Aaij *et al.* (LHCb Collaboration), J. High Energ. Phys. **10**, 086 (2018).
 - [34] A. V. Berezhnoy, A. V. Luchinsky and A. A. Novoselov, Phys. Rev. D **86**, 034004 (2012).
 - [35] A. Esposito and A. D. Polosa, Eur. Phys. J. C **78**, 782 (2018).
 - [36] M. N. Anwar, J. Ferretti, F. -K. Guo, E. Santopinto and B. -S. Zou, Eur. Phys. J. C **78**, 647 (2018).
 - [37] M. A. Bedolla, J. Ferretti, C. D. Roberts and E. Santopinto, arXiv: 1911.00960 [hep-ph].
 - [38] Z. -G. Wang, Eur. Phys. J. C **77**, 432 (2017).
 - [39] W. Chen, H. -X. Chen, X. Liu, T. G. Steele and S. -L. Zhu, Phys. Lett. B **773**, 247 (2017).
 - [40] Y. Bai, S. Lu and J. Osborne, Phys. Rev. B **798**, 134930 (2019).
 - [41] W. Heupel, G. Eichmann and C. S. Fischer, Phys. Lett. B **718**, 545 (2012).
 - [42] V. R. Debastiani and F. S. Navarra, Chin. Phys. C **43**, 013105 (2019).
 - [43] A. V. Berezhnoy, A. K. Likhoded, A. V. Luchinsky and A. A. Novoselov, Phys. Rev. D **84**, 094023 (2011).
 - [44] M. Karliner, S. Nussinov and J. L. Rosner, Phys. Rev. D **95**, 034011 (2017).
 - [45] J. -M. Richard, A. Valcarce and J. Vijande, Phys. Rev. D **95**, 054019 (2017).
 - [46] J. Wu, Y. -R. Liu, K. Chen, X. Liu and S. -L. Zhu, Phys. Rev. D **97**, 094015 (2018).
 - [47] X. Chen, Eur. Phys. J. A **55**, 106 (2019).
 - [48] M. -S. Liu, Qi -F. Lü and X. -H. Zhong and Q. Zhao, Phys. Rev. D **100**, 016006 (2019).
 - [49] G. -J. Wang, L. Meng and S. -L. Zhu, arXiv: 1907.05177 [hep-ph].
 - [50] J. -M. Richard, A. Valcarce and J. Vijande, Phys. Rev. C **97**, 035211 (2018).
 - [51] C. Hughes, E. Eichten and C. T. H. Davies, Phys. Rev. D **97**, 054505 (2018).
 - [52] E. J. Eichten and C. Quigg, Phys. Rev. Lett. **119**, 202002 (2017).
 - [53] M. Karliner and J. L. Rosner, Phys. Rev. Lett. **119**, 202001 (2017).
 - [54] E. Hernández, J. Vijande, A. Valcarce and Jean-Marc Richard, arXiv: 1910.13394 [hep-ph].
 - [55] C. E. Fontoura, G. Krein, A. Valcarce and J. Vijande, Phys. Rev. D **99**, 094037 (2019).
 - [56] J. Carlson, L. Heller and J. A. Tjon, Phys. Rev. D **37**,

- 744 (1988).
- [57] D. Ebert, R. N. Faustov, V. O. Galkin and W. Lucha, Phys. Rev. D **76**, 114015 (2007).
 - [58] L. Leskovec, S. Meinel, M. Pflaumer and M. Wagner, Phys. Rev. D **100**, 014503 (2019).
 - [59] A. Francis, R. J. Hudspith, R. Lewis and K. Maltman, Phys. Rev. Lett. **118**, 142001 (2017).
 - [60] P. Junnarkar, N. Mathur and M. Padmanath, Phys. Rev. D **99**, 034507 (2019).
 - [61] S. S. Agaev, K. Azizi and H. Sundu, arXiv: 1905.07591 [hep-ph].
 - [62] A. Francis, R. J. Hudspith, R. Lewis and K. Maltman, Phys. Rev. D **99**, 054505 (2019).
 - [63] A. Ali, Q. Qin and W. Wei, Phys. Lett. B **785**, 605 (2018).
 - [64] A. Ali, A. Ya. Parkhomenko, Q. Qin and W. Wang, Phys. Lett. B **782**, 412 (2018).
 - [65] G. K. C. Cheung, C. E. Thomas, J. J. Dudek and R. G. Edwards, JHEP **11**, 033 (2017).
 - [66] S. S. Agaev, K. Azizi and H. Sundu, Phys. Rev. D **99**, 114016 (2019).
 - [67] Y. Yang and J. Ping, Phys. Rev. D **99**, 094032 (2019).
 - [68] Z. -G. Wang, arXiv: 1907.10921 [hep-ph].
 - [69] E. Hiyama, Y. Kino and M. Kamimura, Prog. Part. Nucl. Phys. **51**, 223 (2003).
 - [70] A. Valcarce, F. Fernández, P. Gonzalez and V. Vento, Phys. Lett. B **367**, 35 (1996).
 - [71] J. Segovia, D. R. Entem and F. Fernandez, Phys. Lett. B **662**, 33 (2008).
 - [72] J. Segovia, A. M. Yasser, D. R. Entem and F. Fernández, Phys. Rev. D **78**, 114033 (2008).
 - [73] P. G. Ortega, J. Segovia, D. R. Entem and F. Fernández, Phys. Rev. D **94**, 114018 (2016).
 - [74] G. Yang, J. Ping and J. Segovia, Few-Body Syst. **59**, 113 (2018).
 - [75] G. Yang, J. Ping, P. G. Ortega and J. Segovia, arXiv: 1904.10166 [hep-ph].
 - [76] F. Fernandez, A. Valcarce, U. Straub and A. Faessler, J. Phys. G **19**, 2013 (1993).
 - [77] A. Valcarce, F. Fernández, A. Buchmann and A. Faessler, Phys. Rev. C **50**, 2246 (1994).
 - [78] P. G. Ortega, J. Segovia, D. R. Entem and F. Fernández, Phys. Rev. D **81**, 054023 (2010).
 - [79] P. G. Ortega, J. Segovia, D. R. Entem and F. Fernández, Phys. Rev. D **94**, 074037 (2016).
 - [80] P. G. Ortega, J. Segovia, D. R. Entem and F. Fernández, Phys. Rev. D **95**, 034010 (2017).
 - [81] J. Vijande, A. Valcarce and K. Tsushima, Phys. Rev. D **74**, 054018 (2006).
 - [82] G. Yang and J. Ping, Phys. Rev. D **95**, 014010 (2017).
 - [83] G. Yang and J. Ping, Phys. Rev. D **97**, 034023 (2018).
 - [84] G. Yang, J. Ping and J. Segovia, Phys. Rev. D **99**, 014035 (2019).
 - [85] S. Aoyama, T. Myo, K. Kato and K. Ikeda, Prog. Theor. Phys. **116**, 1 (2006).
 - [86] T. Myo, Y. Kikuchi, H. Masui and K. Kato, Prog. Part. Nucl. Phys. **79**, 1 (2014).
 - [87] M. Oka, S. Maeda and Y. -R. Liu, Intl. J. Mod. Phys. **49**, 1960004 (2019).
 - [88] J. Aguilar and J. M. Combes, Commun. Math. Phys. **22**, 269 (1971).
 - [89] E. Balslev and J. M. Combes, Commun. Math. Phys. **22**, 280 (1971).
 - [90] G. S. Bali, H. Neff, T. Duessel, T. Lippert and K. Schilling, Phys. Rev. D **71**, 114513 (2005).
 - [91] M. D. Scadron, Phys. Rev. D **26**, 239 (1982).
 - [92] M. Harvey, Nucl. Phys. A **352**, 326 (1981).
 - [93] J. Vijande, A. Valcarce and N. Barnea, Phys. Rev. D **79**, 074010 (2009).
 - [94] T. F. Caramés, J. Vijande and A. Valcarce, Phys. Rev. D **99**, 014006 (2019).